Rapid Analysis of Förster Resonance Energy Transfer by Two-Color Global Fluorescence Correlation Spectroscopy: Trypsin Proteinase Reaction

Christian Eggeling,* Peet Kask,† Dirk Winkler,† and Stefan Jäger†
*Max-Planck Institute for Biophysical Chemistry, Department of NanoBiophotonics, 37077 Goettingen, Germany; and
†Evotec OAI AG/Evotec Technologies GmbH, 22525 Hamburg, Germany

ABSTRACT In this study we introduce the combination of two-color global fluorescence correlation spectroscopy (2CG-FCS) and Förster resonance energy transfer (FRET) as a very powerful combination for monitoring biochemical reactions on the basis of single molecule events. 2CG-FCS, which is a new variation emerging from the family of fluorescence correlation spectroscopy, globally analyzes the simultaneously recorded auto- and cross-correlation data from two photon detectors monitoring the fluorescence emission of different colors. Overcoming the limitations inherent in mere auto- and cross-correlation analysis, 2CG-FCS is sensitive in resolving and quantifying fluorescent species that differ in their diffusion characteristics and/or their molecular brightness either in one or both detection channels. It is able to account for effects that have often been considered as sources of severe artifacts in two-color and FRET measurements, the most prominent artifacts comprising photobleaching, cross talk, or concentration variations in sample preparation. Because of its very high statistical accuracy, the combination of FRET and 2CG-FCS is suited for high-throughput applications such as drug screening. Employing beam scanning during data acquisition even further enhances this capability and allows measurement times of <2 s. The improved performance in monitoring a FRET sample was verified by following the protease cleavage reaction of a FRET-active peptide. The FRET-inactive subpopulation of uncleaved substrate could be correctly assigned, revealing a substantial portion of inactive or missing acceptor label. The results were compared to those obtained by two-dimensional fluorescence intensity distribution analysis.

INTRODUCTION

Biological assays based on fluorescence detection are one of the most important tools in life science. Fluorescence readouts have gained major attraction not only due to their superior sensitivity to environmental properties and also its multidimensionality, i.e., its ability to provide various simultaneous readouts (e.g., intensity, anisotropy, spectral characteristics), but also due to their ever-growing range of measurement techniques (1). The improvements in the field of confocal microscopy have opened up the door to the direct detection of single molecule events (2–6). This, in turn, made the direct observation of fluctuations in fluorescence emission possible. These fluctuations are otherwise hidden in a large ensemble, but carry valuable information on the dynamics of individual molecules (7). The analysis of fluorescence fluctuations (fluorescence fluctuation spectroscopy (FFS)) tackles the task of molecular resolution, i.e., the unequivocal identification and characterization of different fluorescing molecules. The first FFS method to appear was fluorescence correlation spectroscopy in 1972 (8). Fluorescence correlation spectroscopy (FCS) resolves components with different diffusion coefficients and represents a sensitive tool for biochemical assays rendering a change in mass such as binding studies. However, a difference by a factor of approximately seven in molecular weight is needed to unambitiously distinguish two species (9). Furthermore, a major limitation of FCS as a rapid analysis tool is its statistical decline when going to very short measurement times (10).

Therefore, other FFS methods have been introduced to resolve different species according to their molecular fluorescence brightness (number of detected photons per time interval). Higher order autocorrelation (11) and higher order moment analysis (12) determine the molecular brightness from moments of the fluorescence fluctuations. A successor of these methods was independently developed by Chen et al. (13) and Kask et al. (14). Denoted as photon counting histogram (PCH) and fluorescence intensity distribution analysis (FIDA), respectively, this method calculates the brightness parameter from the statistics on the amplitude (number of photons) axis of the fluorescence fluctuations and has been applied on a variety of biochemical assays (15–17), even involving in vivo studies (18) and industrial applications such as high-throughput drug screening (HTS) (10,19,20). A special adaptation of this approach to single-molecule measurements was highlighted by burst size distribution (BSD) analysis (21).

To improve the statistics and applicability of FCS and FIDA/PCH, both methods were expanded into two dimensions, fluorescence cross-correlation spectroscopy (FCCS) (22,23) and two-dimensional fluorescence intensity distribution analysis (2D-FIDA) (24) or dual-color PCH (25). The second dimension provides for the detection of coincident

Submitted September 9, 2004, and accepted for publication April 18, 2005.

Address reprint requests to Dr. Christian Eggeling, Max-Planck Institute for Biophysical Chemistry, Dept. of NanoBiophotonics, Am Fassberg 11, 37077 Goettingen, Germany. Tel.: 49-551-201-1359; Fax: 49-551-201-1085; E-mail: ceggeli@gwdg.de.

0006-3495/05/07/605/14 $2.00

doi: 10.1529/biophysj.104.052753

information from a second detector, which may represent a different color or a different polarization direction. Both methods, FCCS (26–36) and 2D-FIDA (10,24,37–40), have achieved remarkable results on various assays ranging from binding events to protease cleavage reactions and on HTS implementations (10,19,20,38).

Major efforts are underway to simultaneously use both types of molecular information, diffusion time and brightness, for the characterization of different species and thus to enhance the statistical accuracy of FFS. A combination of temporal and amplitude fluctuation analysis has been realized by fluorescence intensity multiple distribution analysis (FIMDA) (41). However, FIMDA indirectly determines the temporal diffusion characteristics based on differently recorded FIDA data. An ultimate goal is the simultaneous global analysis of FCS and FIDA/PCH-based data, as expressed before (42). Its realization at this point in time is difficult, in as much as the current theories of FCS and FIDA/PCH use quite different assumptions and approximations. Recently, Laurence et al. (43) have introduced a new approach, photon arrival-time interval distribution analysis (PAID), which is very similar to FIMDA and combines properties of both FCS and FIDA/PCH. FIMDA measures fluctuation intensity in terms of random numbers of photons per given time interval. PAID analyzes the intensity in terms of random time intervals needed for counting a given number of photons. PAID theory adequately accounts intensity fluctuations in the time interval between a start and a stop photon and thus dynamically adapts to photon-rich time intervals. It enables molecular resolution on the basis of diffusion, brightness, and coincidence on different detection channels. However, for calculating theoretical curves, a Monte Carlo simulation method is applied. The PAID theory is rather sophisticated and the analysis suffers from long calculation times.

Despite the mentioned drawbacks, FCS features some basic advantages. 1), Besides diffusion properties, the rate constants underlying biochemical reactions can be extracted as long as these result in fluorescence emission changes. Such kinetic information is, for example, not directly accessible by amplitude analysis. 2), FCS was developed in 1972. It is well known and has been extensively applied. 3), The common theory of FCS is based on Gaussian-shaped confocal volumes, which allows one to analytically express theoretical curves for fast and straightforward fitting. 4), In most fluorescence applications, high population densities of triplet states should be avoided. FCS theory and fitting accounts for triplet state population (44). As an example, the control of these effects is possible but still under development for FIDA, as is, for example, outlined in Palo et al. (41). A straightforward approach would allow direct access to the molecular brightness parameter from the correlation curve. This information is in principle contained in its amplitude. Palmer et al. (11) employed the interrelation between (higher order) correlation amplitudes and fluctuation moments to determine the increase in molecular brightness accompanied by aggregation events of a single species. Similar results were obtained from scanning two-photon FCS (45). However, by resolving several components in the autocorrelation function, no direct estimates for molecular concentration, c, and molecular fluorescence brightness, q, but only for their product, cq^2, are obtained. Chen et al. (46) introduced a general approach for the characterization of binding events involving several species with different brightness. Correlation amplitudes were determined from moment analysis. However, a global fit of amplitudes determined from a whole titration experiment was necessary to distinguish bound from unbound species. It is desirable to extract the brightness information from a single correlation experiment and potentially use the simultaneous temporal information as well. In this work, we introduce such an approach based on Förster resonance energy transfer (FRET).

FRET has emerged as one of the most generic homogeneous biological assay principles. In general, FRET constitutes two fluorescence labels with different excitation and emission wavelengths, a donor and an acceptor dye (47). The excitation of the donor dye introduces a certain probability of a nonradiative energy transfer to the acceptor dye and finally leads to its fluorescence emission. The efficiency and therefore the amount of acceptor fluorescence depends on several molecular factors such as the overlap of the donor emission and acceptor excitation spectra, but most importantly on the orientation and the distance between the two dyes. As a consequence, it provides a sensitive tool to resolve distance information of molecular interactions and conformational changes in the range of 1–10 nm. Using FRET, a lot of biological activities involving conformational changes or binding and cleavage reactions can be monitored in detail. For an overview of the whole range of FRET applications, one is referred to recent reports and reviews (3,48–53).

Applying FCS and FCCS to FRET experiments usually requires dual-color detection of donor and acceptor, giving rise to three types of data, two autocorrelation functions (FCS data) and one cross-correlation function (FCCS data). Intensive work has been carried out on studying the impact of FRET on these fluorescence correlation data and how the information of all data can be used to enhance the sensitivity (26,35,54–58). In a recent work, FCS and FRET have been used to analyze conformational changes of single syntaxin 1 molecules (59). The pertaining kinetic time constant was accurately determined by its global use in all three correlation functions. However, as far as we know, a more general global analysis of all three correlation functions has not been applied previously.

This study introduces global analysis of all accessible dual-color FCS and FCCS data (two-color global fluorescence correlation spectroscopy (2CG-FCS)) as a very powerful and rapid tool to analyze the characteristics of FRET fluorescence signals. Amplitude characteristics are subject to global fitting, which can, in principle, be extended

to temporal (diffusion) parameters. Limitations inherent in mere FCS and FCCS analysis can well be compensated. Beside diffusion properties, 2CG-FCS directly determines the molecular concentration and brightness. It accounts for effects like cross talk between the two detection channels, which is common to most FRET experiments. Together with beam scanning, 2CG-FCS is well amenable to industrial applications including HTS, which calls for measurement times <2 s. As an exemplary application, the activity of a trypsin protease reaction is monitored using a peptide substrate labeled on both ends with a green (donor) and a red (acceptor) dye, respectively. Upon cleavage of the substrate by Trypsin, the FRET efficiency and thus the acceptor signal decreases and the kinetics of the enzymatic reaction can be monitored. The obtained results agree with those revealed by the well-established analysis tool 2D-FIDA. Both methods exhibit enough sensitivity to assign the high fraction of a FRET-inactive subpopulation of the uncleaved peptide to substrate molecules with inactive or missing acceptor label.

MATERIALS AND METHODS

Förster resonance energy transfer

In general, energy transfer refers to a process, in which the electronic excitation energy of an excited dye molecule, D^* (donor), is transferred to another dye molecule, A (acceptor), leading to the electronic excitation of the acceptor, A^*, and the deexcitation of the donor, D, $D^* + A \rightarrow D + A^*$. Hence, donor fluorescence is quenched and without direct excitation acceptor fluorescence is formed. Förster resonance energy transfer is one of the most important energy transfer mechanisms and was first theoretically derived by Förster (47). It defines the nonradiative energy transfer from D^* to A via a dipole-dipole interaction. Prerequisites for an efficient Förster resonance energy transfer are: 1), a sufficient overlap of the donor fluorescence emission and acceptor fluorescence excitation spectrum; 2), a spatial distance of ≈1–10 nm of both dyes; 3), a favorable spatial orientation of donor and acceptor dye; and 4), a high donor fluorescence quantum yield. The efficiency of the energy transfer, E, is defined by the induced fluorescence change, i.e., quenching of the donor fluorescence, and shows the characteristic sixth power dependence on the spatial distance, r, between donor and acceptor. This dependence makes FRET such a sensitive tool for many biological reactions including conformational changes or binding and cleavage reactions.

$$E = 1 - \frac{\Phi_{DA}}{\Phi_D} = \frac{1}{1 + (r/R_0)^6} = 1 - \frac{\tau_{DA}}{\tau_D}, \qquad (1)$$

where Φ_D and τ_D are fluorescence quantum yield and lifetime of the donor alone, i.e., in the absence of FRET or acceptor; Φ_{DA} and τ_{DA} are fluorescence quantum yield and lifetime of the donor in the presence of FRET; and R_0 is Förster radius, characteristic for a specific donor acceptor dye pair and their spectroscopic properties, such as spectral overlap of donor emission and acceptor excitation spectrum and orientation of donor and acceptor dipole. A typical value of the Förster radius for the dye molecules in use lies in the range of 1–10 nm (3,48–53).

Optical equipment

As detection system, the EVOTEC FCS+plus spectrometer was used, which basically is a single pinhole confocal fluorescence microscope. The optical scheme of the experiment has been described previously (24). The fluorescence is excited using continuous wave (CW) laser light, a 488-nm CW argon ion laser (JDS-Uniphase, 2014-25MLYVW, San Jose, CA) for direct excitation of the donor dye and for FRET signal generation, and a 633-nm helium-neon laser (JDS-Uniphase, 1135P) for direct excitation of the acceptor dye, which of course was not used in the case of FRET. The exciting light is focused onto the sample by a water-immersion objective lens (U-APO/340, 40×, N.A. 1.15; Olympus Optical, Tokyo, Japan). The fluorescence light is collected by the same objective and passes several optical parts: 1), a two-color dichroic mirror (Omega Optical, Brattleboro, VT) serves to transmit the fluorescence light and reflect the laser light; 2), focusing on a confocal pinhole (70 μm diameter) serves to reject the out-of-focus light; and 3), a dichroic color beam splitter centered at 565 nm (Omega Optical) splits the fluorescence signal onto two avalanche photodiodes (SPCM-AQ-131, Perkin-Elmer Optoelectronics, Fremont, CA) with two different interference filters (535 DF45 and 670 DF40, Omega Optical). Thus, the fluorescence can be monitored in two different wavelength ranges (40–45-nm windows around 535 and 670 nm) defined as the green and red detection channel, respectively. This setup enables the simultaneous recording of the fluorescence signals from the donor (green detection channel) and the acceptor dye (red detection channel). The fluorescence signal is processed online and stored simultaneously as FCS and FCCS (50-ns time resolution), as well as 2D-FIDA (40-μs time window) data. The radius of the monitored sample volume is ≈0.6 μm yielding diffusion times for simple organic dye molecules such as rhodamine green (RhGr) of ≈160 μs in an aqueous solution.

The FCS+plus system allows for scanning of the beam (40 Hz and 100 μm in both radial directions) to minimize photobleaching and increase statistical accuracy due to gathering of more single molecule events in the same amount of time as shown below.

The trypsin assay

Trypsin is a member of a large and diverse family of serine proteases. These enzymes play essential roles in digestion, blood clotting, and cell differentiation, and as regulators through the activation of precursor proteins (60,61). One of the most sensitive methods for the detection of proteolytic activity is FRET. Labeling a substrate at the N- and C-terminus with a donor and acceptor dye, respectively, provides for an ideal FRET conjugate. Cleavage of the conjugate by trypsin will interrupt the FRET signal and hence the kinetics of the reaction can be monitored.

The substrate (NH-Gly-Pro-Ala-Lys-Leu-Ala-Ile-Gly-Lys-$CONH_2$) is labeled with rhodamine green (RhGr, Molecular Probes, Eugene, OR) and MR121 (Roche Diagnostics, Mannheim, Germany) at the N- and C-terminus, respectively. The excitation of the RhGr molecule at 488 nm with its fluorescence emission maximum at 527 nm results in an energy transfer toward the MR121 molecule (excitation maximum at 660 nm, fluorescence emission maximum at 677 nm), because the distance between both dyes is <10 nm. Therefore, the RhGr dye, whose fluorescence is collected in the green detection channel, acts as the donor, and MR121, whose fluorescence is collected in the red detection channel, acts as the acceptor. Once the trypsin is added, the conjugate is cleaved at Lys-Leu (Fig. 1) and the energy transfer is interrupted (62). The cleaved substrate is therefore the FRET-inactive species with a vanished MR121 and a concurrent increased RhGr fluorescence emission. In contrast, the uncleaved substrate is the FRET-active species.

The conjugate (2.5 μM) was incubated at 37°C with trypsin (75 nM) in the following buffer (reaction buffer): 50 mM HEPES pH 8, 100 mM NaCl, 10 mM $CaCl_2$, and 0.05% Pluronic. Aliquots were withdrawn and diluted 1000-fold into buffer (analysis buffer, 5 mM EDTA, 0.5% SDS, 10 mM Tris/HCl, pH 7.8) after 3–60 min of incubation time, yielding different fractions of cleaved peptide and consequently different fluorescence signal in the green and red detection channels. We are applying the substrate concentration far below the K_m-value of ≈60 μM for a Lys-Leu motive (62), to lower the initial reaction rate and, thus, to observe the enzyme reaction with a good time resolution.

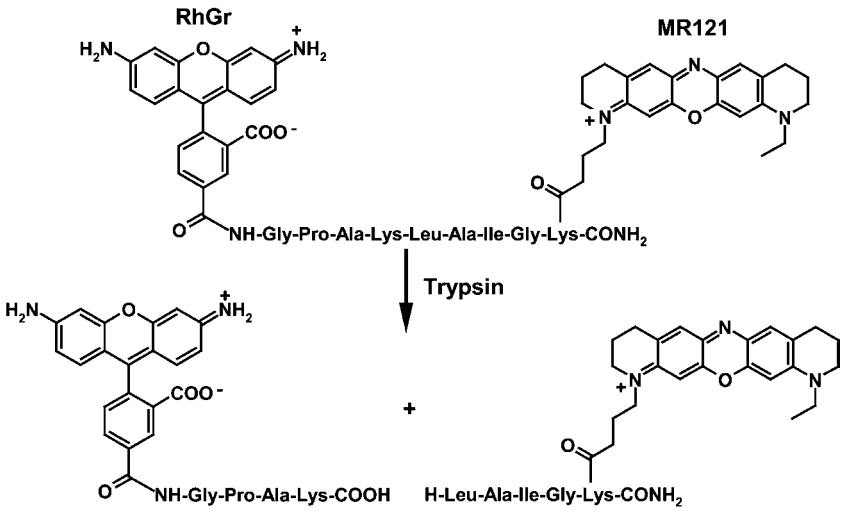

FIGURE 1 Principle of the trypsin assay.

ANALYSIS METHODS

Molecular brightness

The fluorescence emission of the donor or acceptor dyes detected in the green or red detection channel is best expressed by the molecular brightness, q, which is the detected fluorescence count rate per single particle. In the presented FRET experiment, a pair of brightness, q_i^G and q_i^R, one for each detection channel, characterizes each species, i. The index ''G'' denotes the green and the index ''R'' the red detection channel. Furthermore, two species are present, FRET-active substrate (denoted by the index ''on'') and FRET-inactive substrate (denoted by the index ''off''). A close vicinity of active donor and acceptor, characteristic for the uncleaved peptide, characterizes the FRET-active substrate. In contrast, FRET-inactive species are due to an active donor but no acceptor in its vicinity. This is either due to a cleaved substrate or due to an inactive acceptor (a fact that will be discussed later). A potential third species composed of an active acceptor and an absent or inactive donor is practically invisible and not observed. Due to the energy transfer induced by FRET (compare Eq. 1), FRET activity leads to a decrease in donor brightness (green detection channel, q_i^G) and an increase in acceptor brightness (red detection channel, q_i^R). Thus, the fluorescence brightness is an intrinsic molecular parameter characteristic for each of the present species.

Two experimental effects have to be taken into account when monitoring the fluorescence emission in dual-color experiments (26,27,35). 1), Due to the nature of the fluorescence emission spectrum (which decays very slowly toward the red wavelength region), parts of the donor fluorescence can as well be detected in the red detection channel. 2), Due to the nature of the fluorescence excitation spectrum (which decays very slowly toward the blue/short wavelength region), there is a certain possibility of directly exciting the acceptor dye with the 488-nm excitation light and not only via energy transfer. These effects are denoted emission and excitation cross talk and lead to an increase in brightness, q_i^R, of the red (acceptor) detection channel. Besides being characteristic for each fluorescent species present in the sample, the brightness parameters intrinsically carry information of nonideal experimental conditions such as cross talk. Taking these values as an experimental measure thus enables us to take these nonidealities into account. The amount of cross talk is characteristic for the experimental setup (e.g., filters and optical elements used), the average amount of donor fluorescence emission, and the direct excitation efficiency of the acceptor. Throughout the experiment, the amount of cross talk is constant for each species in use, inasmuch as the experimental conditions are kept constant and both emissivity and absorption are intrinsic molecular properties. Thus, the fluorescence brightness holds as an excellent molecular parameter to distinguish between the different species present in the FRET experiment.

Concentrations and trypsin activity

The brightness values as specified in the previous chapters are an intrinsic property of the two species present in this assay. They are not influenced by the trypsin activity. In contrast, cleavage of substrate by trypsin leads to a rise in the concentration (mean number of particles in the detection volume) of FRET-inactive, c_{off}, and a complementary decrease in FRET-active substrate, c_{on}. Because we are applying a substrate concentration (2.5 μM) far below the K_m of 60 μM as previously reported for a Lys-Leu motive (62), the cleavage of the substrate due to trypsin can be approximated by an exponential decrease with incubation time, t, and hence is characterized by the time constant, t_0 (63).

$$c_{on}(t) = c_{on}^0 \exp(-t/t_0) + c_{on}^\infty$$
$$c_{off}(t) = c_{tot} - c_{on}(t) = (c_{tot} - c_{on}^\infty) - c_{on}^0 \exp(-t/t_0), \quad (2)$$

where $c_{tot} = c_{on} + c_{off}$ is total substrate concentration (constant over incubation time, t); c_{on}^∞ is concentration of FRET-active species at infinite incubation time $t = \infty$, a fact that will be discussed later, and $c_{on}^0 + c_{on}^\infty$ is concentration of FRET-active species at time 0, i.e., before incubation by trypsin.

Due to effects such as photobleaching, adsorption, or miss dispensing of the aliquots, the concentration may vary between the samples or measurements (see deviations from a constant line in the inset of Fig. 5 *A*). By using the information from both detection channels at the same time, one can account for this effect and determine the fraction of FRET-active species, which simply applies the normalized concentration, c_{on}/c_{tot}, independent of such variations.

$$\frac{c_{on}(t)}{c_{tot}(t)} = \frac{c_{on}^0}{c_{tot}} \exp(-t/t_0) + \frac{c_{on}^\infty}{c_{tot}}. \quad (3)$$

Fluorescence correlation spectroscopy

In FCS, the fluctuating signal intensities of each single detector are monitored in time and a correlator card or alternatively a software algorithm computes their autocorrelation functions. In contrast, fluorescence cross-correlation spectroscopy studies the cross-correlation function between both channels. For two-color detection, three different correlation functions can be determined, autocorrelation of the signal in the green detection channel, $G_{FCS}^G(t_c)$, autocorrelation of the signal in the red detection channel, $G_{FCS}^R(t_c)$, and cross-correlation of the signal from the green and the red channel, $G_{FCCS}(t_c)$. We apply unnormalized correlation functions, like in the very first studies in the field (8), but in contrast to current studies where normalized functions are preferred (7).

$$G^{G/R}_{FCS}(t_c) = \langle \delta I_{G/R}(t')\, \delta I_{G/R}(t'+t_c)\rangle$$
$$= \langle I_{G/R}(t')\, I_{G/R}(t'+t_c)\rangle - \langle I_{G/R}(t')\rangle\langle I_{G/R}(t')\rangle$$
$$G_{FCCS}(t_c) = \langle \delta I_G(t')\, \delta I_R(t'+t_c)\rangle$$
$$= \langle I_G(t')\, I_R(t'+t_c)\rangle - \langle I_G(t')\rangle\langle I_R(t')\rangle, \quad (4)$$

where t_c is correlation time; $I_{G/R}(t')$ is signal intensity in the green (G) or red (R) detection channel monitored at measurement time, t'; $\langle\rangle$ denotes averaging over measurement time, t'; $\delta I_{G/R}(t') = I_{G/R}(t') - \langle I_{G/R}(t')\rangle$ is fluctuation of the signal at measurement time, t'.

The unnormalized data have proven to be more versatile and adequate for fitting when different species are to be resolved (64).

In its simplest form, the correlation functions decay with a time constant characteristic of the diffusion time of the different fluorescing molecules, i, passing the confocal volume. The amplitudes are a measure of the respective concentrations, c_i, and fluorescence contributions. These contributions are given by the specific brightness of fluorescence, q_i^G and q_i^R, in the green or red detection channel, respectively. The unnormalized functions regarding diffusion and triplet population kinetics of the two fluorescent species present can be expressed as follows (7,23,44).

$$G^G_{FCS}(t_c) = c_{on}\,(q^G_{on})^2\, D^G_{on}(t_c) + c_{off}\,(q^G_{off})^2\, D^G_{off}(t_c) \quad (5a)$$
$$G^R_{FCS}(t_c) = c_{on}\,(q^R_{on})^2\, D^R_{on}(t_c) + c_{off}\,(q^R_{off})^2\, D^R_{off}(t_c) \quad (5b)$$
$$G_{FCCS}(t_c) = c_{on}\,(q^G_{on}q^R_{on})\, D^{FCCS}_{on}(t_c) + c_{off}\,(q^G_{off}q^R_{off})\, D^{FCCS}_{off}(t_c) \quad (5c)$$

$$D^X_i(t_c) = \left(\frac{1}{1+t_c/\rho^X_i}\right)\left(\frac{1}{1+AR^2_X\, t_c/\rho^X_i}\right)^{1/2} + \frac{T^X_i}{1-T^X_i}\exp(-t_c/\mu^X_i),$$

where ρ_i^X is average diffusion time through the detection volume, T_i^X is probability of triplet population, and μ_i^X is triplet correlation time of species, i (on or off), and AR_X is axis ratio of lateral and axial focal expansion, as monitored by the green autocorrelation ($X = G$), the red autocorrelation ($X = R$), and by the cross-correlation ($X = FCCS$) function.

In the case of beam scanning, all correlation functions are influenced by the moving focus. This can be accounted for by modifying the diffusion term, D_i^X (65–70).

$$D^X_i(t_c) = \left(\frac{1}{1+t_c/\rho^X_i}\right)\left(\frac{1}{1+AR^2_X\, t_c/\rho^X_i}\right)^{1/2}\left[(1-A_{scan}) + A_{scan}\exp\left(-\frac{(t_c/t_{scan})^2}{1+t_c/\rho^X_i}\right)\right] + \frac{T^X_i}{1-T^X_i}\exp(-t_c/\mu^X_i). \quad (5d)$$

The variable t_{scan} represents the average scan time of the focal volume. Its value will be slightly higher than solely given by the scanning rate of ~40 Hz ($t_{scan} \approx 2/40$ Hz = 5 ms), inasmuch as the beam is moved back and forth. An approximation is introduced to account for the de- and acceleration periods induced by this movement. Parts of the diffusion term are assumed unaffected by scanning as expressed by the amplitude parameter A_{scan}.

The expressions of Eq. 5 are less familiar. On one hand, usual FCS analysis constitutes normalized data. Normalization is thereby performed by the square of the total fluorescence count rates, $(\sum c_i q_i)^2$, and results in the well-known relation, $G_{FCS}(t_c) = 1/cD(t_c)$, for a single species. In contrast, the amplitude of the unnormalized correlation data increases with increasing fluorophore concentration. Furthermore, in contrast to Widengren et al. (44), the triplet term is added to the diffusion term. Inasmuch as the population and depopulation of the triplet state occurs on a much faster timescale (μ_i^X = 1–2 μs) as well as independently from diffusion or scanning ($\rho_i^X > 150$ μs, $t_{scan} = 6$ ms), it can be treated separately in theory.

FCS and FCCS alone do not enable to directly extract the concentration, c_{off} and c_{on}, but rather the respective amplitudes, $c_i(q_i^G)^2$,$c_i(q_i^R)^2$, or $c_i(q_i^G q_i^R)$.

Two-color global fluorescence correlation spectroscopy

For two-color global FCS analysis, the three correlation functions recorded at the same time are fitted simultaneously using Eq. 5 hereby applying the concentration, $c_{on/off}$, as well as the four brightness parameters, $q^{G/R}_{on/off}$, as global variables. The brightness and all diffusion times and triplet parameters of both species, as well as the axis ratios are predetermined from control experiments of samples containing only uncleaved or maximal cleaved substrate and subsequently fixed to determine the concentration of FRET-active and -inactive substrate over incubation time. The use of the brightness parameters ($q^{G/R}_{on/off}$) for the characterization of each species takes impacts due to cross talk into account. Thus, the normalization, c_{on}/c_{tot} (compare Eq. 3), is a direct monitor of the trypsin activity with a complete correction of the cross talk and concentration effects mentioned above.

Examples of this global correlation analysis are given in Fig. 2.

Two-dimensional fluorescence intensity distribution analysis

Two-dimensional fluorescence intensity distribution analysis relies on the collection of photon count numbers, n_G and n_R, simultaneously recorded in time intervals of fixed duration on two detectors monitoring, e.g., different colors as in this assay (G is green and R is red). These numbers are used to build up a joint distribution of photon count numbers, $P(n_G, n_R)$. A theoretical distribution is fitted to this two-dimensional histogram, yielding molecular concentrations, c_i (mean number of molecules in the detection volume), and a pair, q_i^G and q_i^R, of specific fluorescence brightness values of the first (green) and second (red) detection channel for all different fluorescent species, i, of the sample. In this way, the overall detected signal, I_G and I_R, is split up. Fluorescent compounds of a sample as well as background signal, B_G and B_R, can be resolved on the molecular level, as long as these components display different values for molecular fluorescence brightness on one of the detectors, such as FRET-active and -inactive species.

$$\begin{pmatrix} I_G \\ I_R \end{pmatrix} = \sum c_i \begin{pmatrix} q_i^G \\ q_i^R \end{pmatrix} + \begin{pmatrix} B_G \\ B_R \end{pmatrix} = c_{on}\begin{pmatrix} q^G_{on} \\ q^R_{on} \end{pmatrix} + c_{off}\begin{pmatrix} q^G_{off} \\ q^R_{off} \end{pmatrix} + \begin{pmatrix} B_G \\ B_R \end{pmatrix}. \quad (6)$$

As a result, 2D-FIDA gives more statistical reliability for biological assays, because compounds are differentiated and background signals, originating in cross talk or autofluorescing compounds, are accounted for. A detailed description of 2D-FIDA is given elsewhere (24,71).

Here the brightness values of the two species present are predetermined from control experiments of samples containing only uncleaved or maximal cleaved substrate and subsequently fixed to determine the concentration of FRET-active and -inactive substrate over incubation time. By normalization, c_{on}/c_{tot}, the trypsin activity is followed using Eq. 3 with a complete correction with respect to the cross talk and concentration effects as mentioned above.

RESULTS

FCS, FCCS, and 2D-FIDA data were recorded simultaneously. Measurements have been performed for 2 s using

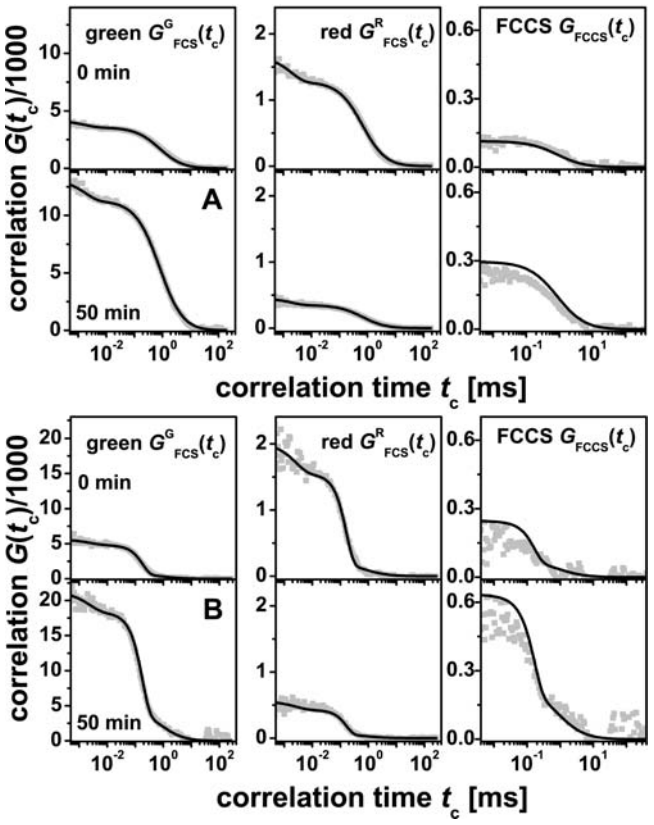

FIGURE 2 Exemplary 2CG-FCS data without (*A*) and with (*B*) beam scanning after 0 min (*top graphs*) and 50 min (*bottom graphs*) incubation by trypsin; autocorrelation data of green, $G^G_{FCS}(t_c)$, and red, $G^R_{FCS}(t_c)$, detection channel and cross-correlation data, $G_{FCCS}(t_c)$ (FCCS), (*gray dots*) with according 2CG-FCS fit (*black line*).

beam scanning and for 10 s without beam scanning. Statistical significance was induced by 10-fold repetition of each sample prepared. Laser light of 488 nm and an irradiance of 90 kW/cm^2 was used to evoke fluorescence excitation.

Background signal due to Rayleigh and Raman scattering and detector dark counts amounted to 2.5 kHz for the green and 0.2 kHz for the red detection channel, respectively. In 2D-FIDA, the background was accounted for by an additional (fixed) component. Because the lowest count rate was 90 kHz in the case of the green and 10 kHz in the red detection channel (i.e., signal/background ratios of 36 and 50, respectively), the contribution of the background is negligible in FCS and FCCS.

Fluorescence correlation spectroscopy

At first, standard fluorescence correlation spectroscopy (FCS) analysis was applied to the autocorrelation data recorded in the green as well as in the red detection channel. Fig. 2 shows exemplary FCS data for samples containing only uncleaved (0 min) and maximal cleaved substrate (50 min). FRET activity can be followed by a decreased amplitude of the green and an increased amplitude of the red autocorrelation data in the case of uncleaved substrate, because unnormalized correlation curves are used and because the concentration of FRET-active species, c_{on}, decreases with incubation time at the expense of FRET-inactive species, c_{off} ($q^G_{off} > q^G_{on}$ and $q^R_{on} > q^R_{off}$; compare Eq. 5). The FCS data were fitted by the according expressions of Eqs. 5a and 5b (including Eq. 5d for experiments applying beam scanning). The diffusion times, triplet parameters, axis ratios, and scanning parameters were determined from data of samples containing pure uncleaved or maximal cleaved substrate. Their values are listed in Table 1. The diffusion times as well as triplet parameters are, however, indistinguishable for FRET-active and -inactive substrate (i.e., $D^{G/R}_{on}(t_c) = D^{G/R}_{off}(t_c)$). This takes away potential parameters to discriminate the two species and, thus, decreases sensitivity of any FCS analysis, which is on a major part based on diffusion times. On the other hand, it offers to slightly simplify Eqs. 5a and 5b. Insertion of Eq. 2 expresses the time course of the according FCS amplitudes, $G^G_{FCS}(0)$ and $G^R_{FCS}(0)$, with incubation time, t.

$$G^{G/R}_{FCS}(t_c) = \left[c_{on}\left(q^{G/R}_{on}\right)^2 + c_{off}\left(q^{G/R}_{off}\right)^2\right] D^{G/R}(t_c) = G^{G/R}_{FCS}(0)\, D^{G/R}(t_c), \quad (7)$$

with $G^G_{FCS}(0) = B_G + A_G \exp(-t/t_0)$ and $G^R_{FCS}(0) = B_R + A_R \exp(-t/t_0)$; $D^{G/R}(t_c) = D^{G/R}_{on}(t_c) = D^{G/R}_{off}(t_c)$; $A_{G/R} = c^0_{on}[(q^{G/R}_{on})^2 - (q^{G/R}_{off})^2]$; $B_{G/R} = c^\infty_{on}[(q^{G/R}_{on})^2 - (q^{G/R}_{off})^2] + c_{tot}(q^{G/R}_{off})^2$. Thus, an exponential rise is expected for the green $\left(q^G_{off} > q^G_{on}\right)$ and a decay for the red detection channel $\left(q^R_{off} < q^R_{on}\right)$.

With the diffusion time, triplet parameter, axis ratio, and scanning parameters fixed to the values determined from the control experiments (Table 1), the estimated amplitudes, $G^G_{FCS}(0)$ and $G^R_{FCS}(0)$, are plotted against incubation time, t (Fig.3). The amplitudes are severely biased by the variations in concentration from sample to sample, which are by far largerthan the standard deviation of a single measurement. We assume these variations are due to glass adsorption, miss dispensing, and/or photobleaching, as will be further outlined below. As a consequence of the sample-to-sample variations, a fit of Eq.7 to the data only yields very imprecise results as stated in Table1. These effects might be compensated by a method that simultaneously uses the information from both detection channels, such as two-color ratio FCS analysis or fluorescence cross-correlation spectroscopy.

Two-color ratio FCS analysis

An easy way to express the information obtained by FCS from the green and red detection channel simultaneously is to investigate the ratio of the amplitudes of the two autocorrelation data, R_{FCS} (compare Eq. 7).

TABLE 1 Values of the trypsin assay as determined by FCS (and two-color ratio FCS), FCCS, 2CG-FCS, and 2D-FIDA

		FCS green	FCS red	FCCS	2D-FIDA	2CG-FCS
FRET-active	q_{on}^{G} (kHz)					
	(+bs)	*	*	*	0.5 ± 0.2	1.5 ± 0.4
	(−bs)	*	*	*	0.2 ± 0.1	0.5 ± 0.3
	q_{on}^{R} (kHz)					
	(+bs)	*	*	*	27 ± 1	27.3 ± 0.7
	(−bs)	*	*	*	27 ± 1	28.5 ± 1
	ρ_{on} (μs)					
	(+bs)	†	†	†	*	‡
	(−bs)	810 ± 80	680 ± 90[§]	890 ± 100	*	‡
	T_{on}					
	(+bs)	0.14 ± 0.02	0.23 ± 0.05	0	*	‡
	(−bs)	0.14 ± 0.02	0.23 ± 0.05	0	*	‡
	μ_{on} (μs)					
	(+bs)	1.8 ± 0.6	2.0 ± 0.7	*	*	‡
	(−bs)	1.8 ± 0.6	2.0 ± 0.8	*	*	‡
FRET-inactive	q_{off}^{G} (kHz)					
	(+bs)	*	*	*	41 ± 1	42.1 ± 3
	(−bs)	*	*	*	38 ± 1	39 ± 1
	q_{off}^{R} (kHz)					
	(+bs)	*	*	*	1.2 ± 0.1	1.4 ± 0.3
	(−bs)	*	*	*	1.1 ± 0.1	1.0 ± 0.2
	ρ_{off} (μs)					
	(+bs)	¶	¶	¶	*	‡
	(−bs)	¶	¶	¶	*	‡
	T_{off}					
	(+bs)	¶	¶	¶	*	‡
	(−bs)	¶	¶	¶	*	‡
	μ_{off} (μs)					
	(+bs)	¶	¶	¶	*	‡
	(−bs)	¶	¶	¶	*	‡
Axis ratio	AR					
	(+bs)	†	†	†	*	‡
	(−bs)	3.5 ± 0.8	3.5 ± 0.7	3.5 ± 1.0	*	‡
Trypsin activity	t_0 (min)					
	(+bs)	15 ± 10 10.6 ± 0.6[‖]	15 ± 12	9 ± 8	12.4 ± 0.7	12.5 ± 0.9
	(−bs)	20 ± 10 12.5 ± 0.6[‖]	20 ± 8	13 ± 11	14.0 ± 0.9	14.3 ± 0.8
Statistical accuracy	Z'					
	(+bs)**	†† 0.91[‖]	††	††	0.97	0.91
	(−bs)‡‡	†† 0.90[‖]	††	††	0.93	0.89

The values result from the analysis of control measurements of pure uncleaved and maximal cleaved substrate, from the dependence of the according data on the incubation time (cleavage time t_0), and of the corresponding Z'-values (Eq. 11) for the different analysis methods with (+bs) and without (−bs) beam scanning.

*Parameter not determined by this method.

†The diffusion term is modified according to Eq. 5d; diffusion time and axis ratio were fixed to $\rho_i^X = 810\,\mu$s and $AR = 3.5$ and scanning parameters determined to be $t_{scan} = 6 \pm 0.5$ ms and $A_{scan} = 0.8 \pm 0.05$ in all cases.

‡These parameters of 2CG-FCS were taken from the respective FCS and FCCS analysis (see text).

§This is an apparent diffusion time, which is shorter than the real diffusion time due to significant photobleaching of the acceptor (compare reference Eggeling (75)).

¶Parameters undistinguishable for FRET-active and -inactive substrate.

‖Determined from the two-color ratio FCS data.

**Measurement time of 2 s.

††Not determinable due to variations in concentration from sample to sample.

‡‡Measurement time of 10 s.

$$R_{FCS} = \frac{G_{FCS}^{R}(0)}{G_{FCS}^{G}(0) + G_{FCS}^{R}(0)} = \frac{A_R \exp(-t/t_0) + B_R}{(A_G + A_R)\exp(-t/t_0) + (B_G + B_R)}. \quad (8)$$

Fig. 4 *A* depicts the decay of the ratio R_{FCS} with incubation time, t, which is free of the sample-to-sample noise present in the pure FCS data. Obviously, the concurrent information of both detection channels is sufficient enough to compensate for the sample-to-sample variation in concentration.

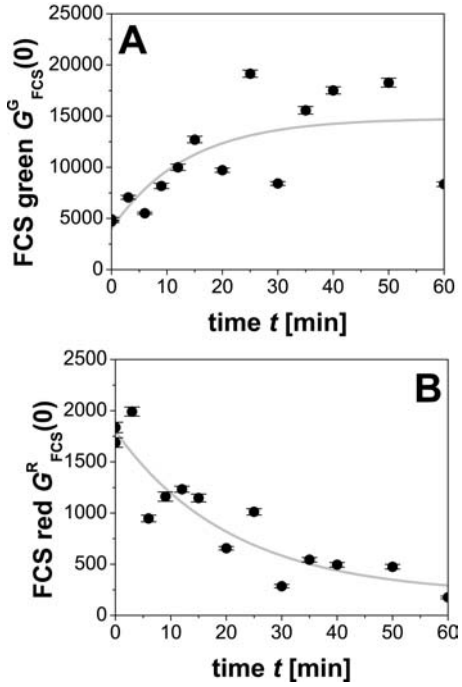

FIGURE 3 Trypsin activity monitored by FCS in the green (*A*) and red (*B*) detection channel with the use of beam scanning; autocorrelation amplitudes, $G^{G}_{FCS}(0)$ and $G^{R}_{FCS}(0)$, respectively, over incubation time, t, and according exponential fit of Eq. 7 to the data (*gray line*): (*A*) $B_G = 14{,}800 \pm 2300$, $A_G = -10{,}800 \pm 3100$, $t_0 = 15 \pm 10$ min; (*B*) $B_R = 200 \pm 180$, $A_R = 1600 \pm 250$, $t_0 = 15 \pm 12$ min.

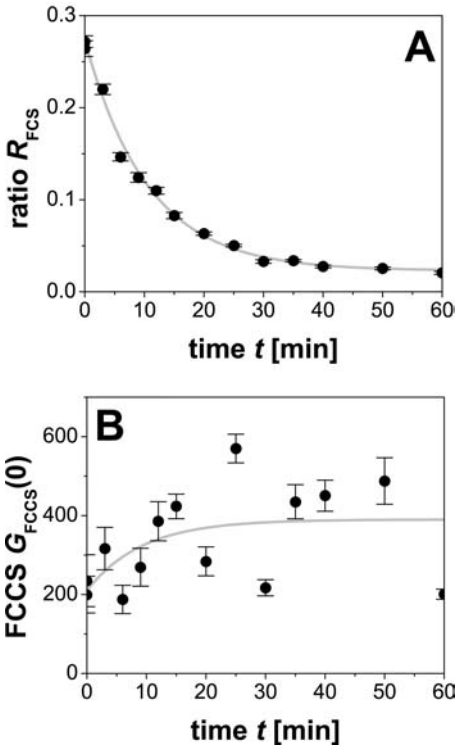

FIGURE 4 Trypsin activity monitored by two-color ratio FCS (*A*) and FCCS (*B*) with the use of beam scanning; ratio, R_{FCS}, and amplitude, $G_{FCCS}(0)$, over incubation time, t, and according exponential fit of Eqs. 9 and 10, respectively, to the data (*gray line*): (*A*) $c^{\infty}_{on}/c_{tot} = 0.023 \pm 0.004$, $c^{0}_{on}/c_{tot} = 0.25 \pm 0.01$, $t_0 = 10.6 \pm 0.6$ min, (*B*) $B_{FCCS} = 390 \pm 55$, $A_{FCCS} = -180 \pm 100$, $t_0 = 9 \pm 8$ min.

However, it is impossible to fit the data using Eq. 8 without prior knowledge of some parameters (e.g., $q^{G/R}_{on}$ and $q^{G/R}_{off}$). Only rude assumptions of no cross talk ($q^{R}_{off} \approx 0$), $q^{R}_{on} \approx q^{G}_{off}$, and 100% FRET efficiency ($q^{G}_{on} \approx 0$) lead to a simplified expression.

$$R_{FCS} = \frac{c^{0}_{on}}{c_{tot}} \exp(-t/t_0) + \frac{c^{\infty}_{on}}{c_{tot}}. \quad (9)$$

This expression fits the data very well, as shown in Fig. 4 *A*. However, due to the incorrect assumptions, the resulting time constant, t_0, is biased (as can be seen from comparison to the results obtained by 2CG-FCS and 2D-FIDA).

Fluorescence cross-correlation analysis

Standard FCCS data were recorded as cross-correlation of the fluorescence signal from the green and red detection channel. Exemplary data are presented in Fig. 2 for uncleaved (0 min) and maximal cleaved substrate (50 min). In as much as the diffusion times as well as triplet parameters are indistinguishable for FRET-active and -inactive substrate (as mentioned in the previous chapter), Eq. 5c is simplified using Eq. 2, expressing the time course of the FCCS amplitude, $G_{FCCS}(0)$, with incubation time, t.

$$\begin{aligned} G_{FCCS}(t_c) &= \left[c_{on}\left(q^{G}_{on}q^{R}_{on}\right) + c_{off}\left(q^{G}_{off}q^{R}_{off}\right)\right] D^{FCCS}(t_c) \\ &= G_{FCCS}(0)\, D^{FCCS}(t_c), \end{aligned}$$

with

$$\begin{aligned} &G_{FCCS}(0) = B_{FCCS} + A_{FCCS}\exp(-t/t_0) \\ &D^{FCCS}(t_c) = D^{FCCS}_{on}(t_c) = D^{FCCS}_{off}(t_c); \\ &A_{FCCS} = c^{0}_{on}\left[\left(q^{G}_{on}\,q^{R}_{on}\right) - \left(q^{G}_{off}\,q^{R}_{off}\right)\right]; \\ &B_{FCCS} = c_{tot}\left(q^{G}_{off}\,q^{R}_{off}\right) + c^{\infty}_{on}\left[\left(q^{G}_{on}\,q^{R}_{on}\right) - \left(q^{G}_{off}\,q^{R}_{off}\right)\right]. \quad (10) \end{aligned}$$

With the diffusion time, triplet parameter, axis ratio, and scanning parameters fixed to the values determined from the control experiments (Table 1), the estimated $G_{FCCS}(0)$ is plotted against incubation time (Fig. 4 *B*). Variations in the concentration from sample to sample once again strongly bias the data. Consequently, a fit of Eq. 10 to the data only yields very imprecise results as stated in Table 1. FCCS is unfavorable in this particular case, because the donor fluorescence is almost completely quenched by FRET (almost 100% FRET efficiency as shown by 2CG-FCS). In principle, there should be no fluorescence emission of the acceptor in the absence of FRET ($q^{R}_{off} = 0$), resulting in $G_{FCCS}(0) = 0$ at infinite incubation time. Consequently,

with a FRET efficiency of 100% ($q^{G}_{on} \approx 0$) one would expect no cross-correlation signal at all at any time, t. However, $G_{FCCS}(0)$ rises with incubation time, t. Thus, the coinciding signal in both detection channels is solely due to the rather weak cross talk. Cross talk is in this case the only cause of the presence of cross-correlated signal. FRET systems, which exhibit less efficiency and, thus, higher brightness values of the donor (e.g., >5 kHz), have already yielded much better results for FCCS (57). This highlights the demand for a method capable of directly determining the molecular concentrations, $c_{on}(t)$ and $c_{off}(t)$, as done by 2CG-FCS.

Two-color global fluorescence correlation spectroscopy

In 2CG-FCS, all three correlation curves, autocorrelation of green and red detection channel and their cross-correlation, are globally analyzed with common parameters, c_i and $q^{G/R}_i$. All parameters that are not subject to global fitting were taken from the single auto- and cross-correlation analysis, i.e., the diffusion times, triplet parameters, and axis ratios, as listed in Table 1, and were fixed throughout the analysis. In this way, the pair of brightness values for each species could be determined from the control measurements of samples containing pure uncleaved and maximal cleaved substrate, which are as well listed in Table 1. FRET is observed by a decrease in green and a concurrent increase in red brightness. From the values of brightness, $q^{G}_{on} = 1.0 \pm 0.3$ kHz and $q^{G}_{off} = 42.5 \pm 3$ kHz, of the donor on FRET-active and -inactive substrate, a FRET efficiency, $E = \left(1 - q^{G}_{on}/q^{G}_{off}\right) = 0.98 \pm 0.007$ (Eq. 1), of close to one is determined. Thus, the donor fluorescence is almost completely quenched in the case of FRET activity.

Examples of 2CG-FCS data and fitting results are presented in Fig. 2. It demonstrates that all three correlation curves can very well be fitted globally. The slightly imperfect description of the FCCS data is probably caused by an incomplete overlap of the green and red detection volume.

A two-component global analysis of all correlation data with brightness fixed to the predetermined values reveals the time course of the concentration, $c_{off}(t)$, as shown in Fig. 5 *A* (*cross*). To check if the variations in concentration from sample to sample are caused by the mentioned concentration effects due to sample handling variations, the inset of Fig. 5 *A* plots the total concentration, $c_{tot} = c_{on}(t) + c_{off}(t)$, for this measurement series (*cross*) as well as for a measurement series taken on another day (*diamonds*). The strong fluctuation in c_{tot}, which is by far larger than the standard deviation of a single measurement, as well as the difference in fluctuation from day-to-day measurements makes it reasonable to assume that the variations are indeed not caused by the trypsin assay or by imprecise data analysis but by sample handling errors.

The concentration effects can be accounted for by calculating the ratio, $c_{on}/(c_{on} + c_{off})$ (Eq. 3, *cross* in Fig. 5 *B*),

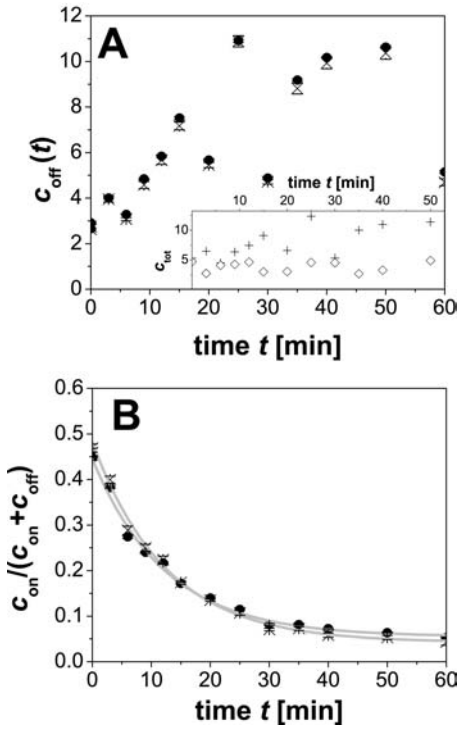

FIGURE 5 Trypsin activity monitored by 2CG-FCS (*cross*) and 2D-FIDA (●) with the use of beam scanning plotted against incubation time, t. (*A*) Concentration values of FRET-inactive substrate, $c_{off}(t)$. (*A*, *inset*) Total concentration, $c_{tot} = c_{on}(t) + c_{off}(t)$, obtained by 2CG-FCS for this measurement series (×) and for another measurement series (◇). (*B*) Ratio, $c_{on}/(c_{on} + c_{off})$, with a fit to the data using Eq. 3 (*gray line*) resulting in the following parameters. 2CG-FCS: $c^{0}_{on}/c_{tot} = 0.44 \pm 0.01$, $c^{\infty}_{on}/c_{tot} = 0.042 \pm 0.007$, $t_0 = 12.5 \pm 0.9$ min. 2D-FIDA: $c^{0}_{on}/c_{tot} = 0.39 \pm 0.01$, $c^{\infty}_{on}/c_{tot} = 0.055 \pm 0.006$, $t_0 = 12.4 \pm 0.7$ min.

which gives an unbiased result of the trypsin activity, t_0, as given in Table 1. It shows that 2CG-FCS can very well be applied to the analysis of FRET assays, despite effects such as cross talk, sample-to-sample variation in concentration, as well as undistinguishable diffusion times.

2D-FIDA

The well-established analysis method 2D-FIDA was applied to prove the validity of the results obtained by 2CG-FCS. In 2D-FIDA, all fluorescent species of the sample can be characterized and distinguished by two parameters, molecular brightness in the green and red detection channel. From the control measurements of samples containing pure uncleaved or maximal cleaved substrate, once again two pairs of brightness values were determined for the species present as given in Table 1. They agree very well with those of 2CG-FCS. A two-component analysis of the 2D-FIDA data with the brightness values fixed to the values given in Table 1 yields a time course of the corresponding concentration, $c_{off}(t)$, as shown in Fig. 5 *A* (*solid circles*). The time dependence of the ratio, $c_{on}/(c_{on} + c_{off})$ (*solid circles* in Fig. 5 *B*), can also be described by Eq. 3 to yield an

unbiased value of the trypsin activity, t_0, as given in Table 1. All results match with those of 2CG-FCS.

Trypsin activity

Table 1 shows the results for t_0 obtained for 2CG-FCS with (and without) beam scanning. With an assumed Michaelis constant, $K_M = 60\ \mu M$, as known for a Lys-Leu motive (62), a maximum reaction velocity, $V_{max} = 0.08 \pm 0.01\ \mu M/s$, is calculated ($V_{max} = K_M/t_0$) (63). Using the trypsin concentration of 75 nM, a value of $k_{cat} = 1.1 \pm 0.1\ s^{-1}$ ($k_{cat} = V_{max}$ / 75 nM) is determined. Kurth et al. calculated values from 0.8 to 40 s^{-1}, depending on the substrate (72). Because in this study a much lower substrate concentration was used (note that K_M is $\approx$60 μM for a Lys-Leu motive and hence a factor of 24 higher than the substrate concentration used in this study), the value of k_{cat} resides within the very low range of expected values (62,72). It is conceivable that the reaction buffer containing detergent (0.05% Pluronic) might retard the cleavage reaction.

The trypsin activity seems to be incomplete, as one might conclude from the residual FRET-active substrate concentration observed at infinite incubation time, $c^{\infty}_{on}/c_{tot} = 5\%$ (Fig. 5 *B*). This cannot be explained by an insufficient cleavage reaction of trypsin, because the reaction buffer conditions in principle are perfect for trypsin activity (62,72). The reaction buffer might retard the reactivity, as outlined above, but should not result in an incomplete cleavage. However, the relative high concentration of SDS (0.5%) in the analysis buffer of the aliquots, which is necessary for a FRET- and acceptor-active substrate conformation, yields substrate enriched detergent micelles. This becomes obvious by a significantly enlarged diffusion time of the substrate in the presence of SDS ($\rho^{G}_{on/off} = 810\ \mu s$), compared to the absence of SDS ($\rho^{G}_{on/off} = 280\ \mu s$) as measured by FCS. Thus, cleaved peptide residing in close vicinity within the same detergent micelle might still exhibit a residual FRET activity.

Beam scanning and photobleaching

Photobleaching is an effect that deteriorates any fluorescence analysis. Due to an enhanced reactivity of the excited fluorophore, it irreversibly loses its fluorescence emission feature, i.e., it is photobleached (73). Because the photobleaching reaction occurs from the excited state of the fluorophore, the probability increases with excitation irradiance and observation time (74). Photobleaching has a misleading effect for fluorescence detection, because it leads to a decrease in detected fluorescence emission by a decline in the fluorescence brightness, i.e., number of emitted photons per single fluorophore, and/or in the concentration, i.e., mean number of fluorophores in the detection volume (73). The effect is severe for any FRET experiment, in as much as donor and acceptor have different photobleaching characteristics. In most cases, the acceptor bleaches faster, which leads to an underestimation of the concentration of FRET-active species (75).

To correct for the effect of photobleaching, the beam scanning option of the instrumentation was employed. Thereby, the beam is moved back and forth in both radial directions over the sample. The movement minimizes the observation time and thus the probability of photobleaching (65,67–70). This can be observed by comparing the determined brightness and concentration values with ($q^{G}_{off} =$ 42.5 kHz; $q^{R}_{on} = 28$ kHz; $c_{tot} = 7 \pm 3$) and without beam scanning ($q^{G}_{off} = 39$ kHz; $q^{R}_{on} = 28.5$ kHz; $c_{tot} = 4 \pm 2$). As shown, beam scanning is well applicable to 2CG-FCS data.

Statistical accuracy for HTS

To evaluate the statistical accuracy of the analysis methods in high-throughput drug screening applications, the Z'-factor is calculated from the samples with uncleaved and maximal cleaved substrate (76). The usage of this factor is widespread in HTS, because it reflects both the assay signal dynamic range and the data variation associated with the measurement and analysis of the according method (10,19,38). With $s_{t=0}$ and $s_{t=60}$ being the readout values of each analysis method ($G^{G/R}_{FCS}(0)$, R_{FCS}, $G_{FCCS}(0)$, $c_{on}/(c_{on} + c_{off})$) at time 0 min and 60 min and denoting $\sigma(s)$ as the standard deviation of the according readout, the Z'-factor is a dimensionless statistical characteristic.

$$Z' = 1 - \frac{3\,\sigma(s_{t=0}) + 3\,\sigma(s_{t=60})}{|s_{t=0} - s_{t=60}|}. \qquad (11)$$

Its maximal value is one and due to its dependence on $\sigma(s)$, it is inversely proportional to the square root of the measurement time. Any screening application is rated sufficiently robust if $Z' > 0.5$. Measurement times in high throughput applications are usually limited to two seconds or below. 2CG-FCS yields a very high Z'-value of 0.91 at the 2-s measurement time, which is almost as good as that reached by the well-established HTS method 2D-FIDA ($Z' = 0.97$). Statistical accuracy is well enhanced by beam scanning. Although the experiments without beam scanning were performed with a five times longer data acquisition time, which should increase accuracy, the Z'-factor is about the same. On one hand this is induced by the lowered photobleaching probability and on the other hand due to gathering of more single molecule events and thus more molecular information in the same amount of time. Although the correlation data may look noisier in the case of beam scanning (compare Fig. 2), the analysis of the correlation amplitude is more accurate. The increased molecular information content is for example expressed by the increase of the correlation amplitudes. The determination of diffusion times will probably be more inaccurate in the case of applying beam scanning.

The very high Z'-values suggest to even further lower the measurement time, which makes 2CG-FCS very attractive

for HTS. We have to note that an assay, which in addition to brightness changes also features differences in diffusion times, would probably further enhance the statistical accuracy of 2CG-FCS.

Fraction of FRET-inactive substrate at incubation time 0

Approximately 45–50% of all original, uncleaved substrates at incubation time, $t = 0$, are FRET inactive, as displayed in Fig. 5 *B*. This feature becomes obvious in a lot of single-molecule experiments (75,77,78). To study this feature in more detail, the concentration and brightness values of FRET-active and FRET-inactive substrate were compared using 2D-FIDA when applying only 488 nm, only 633 nm, and simultaneous 488 and 633 nm excitation at lower irradiances (50 kW/cm^2 (488 nm) and 40 kW/cm^2 (633 nm)) and beam scanning to minimize photobleaching. Thereby, two effects were considered as proven by measurements on single dye solutions of RhGr and MR121. I), Due to an enhanced photobleaching of MR121 by the 488-nm laser light (75), its concentration decreases by ≈25% when adding 488-nm light to 633-nm excitation. II), The focal volume of the 633-nm laser is larger than that of the 488-nm laser by a factor of ≈1.45 as determined from the diffusion times, ρ, resulting from FCS. Because the determined concentration, c, which is the mean number of particles in the detection volume, is directly proportional to the size of the detection volume, the same molar concentration yields a 1.45 times higher mean number of particles in the case of 633-nm excitation. A close inspection of the FRET-active and -inactive subpopulations (with measurements on a sample solely containing uncleaved substrate) indicates the existence of a substantial portion of substrate molecules with inactive or missing acceptor according to the following observations:

1. FRET- (or MR121 fluorescence) inactive substrate. The concentration $c_{\text{off}} = 4.0 \pm 0.2$ as well as the brightness, $q^{\text{G}}_{\text{off}} = 7.9 \pm 0.1$ kHz and $q^{\text{R}}_{\text{off}} = 0.2 \pm 0.1$ kHz, stay constant, regardless of 488-nm or simultaneous 488- and 633-nm excitation; 633-nm excitation leads to no detectable FRET-inactive species. This indicates, that an inactive or missing MR121 label causes the inactivity.
2. FRET- (or RhGr and MR121 fluorescence) active substrate. Going from 633-nm to simultaneous 633- and 488-nm and subsequently to solely 488-nm excitation, the concentration decreases by 25% (from $c = 3.7$ to $c = 2.8$) and subsequently declines by a factor of 1.4 to $c = 2.0$. Concurrently the brightness almost stays constant in the green detection channel ($q^{\text{G}}_{\text{off}} = 0$–$0.5$ kHz) and in the red detection channel it changes from $q^{\text{R}}_{\text{off}} = 22$ to 29 to 11 kHz. The changes in the brightness values can be interpreted by the addition of direct red or simultaneous red and FRET excitation of the MR121 fluorophore. The change in concentration matches the mentioned additional photobleaching (25%) and detection volume size (factor 1.45). This indicates that the real concentration of FRET- (or RhGr and MR121 fluorescence) active species remains constant regardless of the excitation mode.

As a result, the percentage of FRET-inactive uncleaved substrate is either due to an inactive or missing acceptor label.

CONCLUSION

We have introduced two-color global fluorescence correlation analysis as a new method for analyzing FRET assays. 2CG-FCS globally analyzes all accessible dual-color correlation data, i.e., two autocorrelation curves and one cross-correlation curve. As an example, the trypsin protease activity was determined by monitoring the cleavage reaction of a FRET-active peptide. The obtained results coincide with those extracted from the established method 2D-FIDA and compensate limitations inherent in mere FCS and FCCS analysis. Still implying the general advantages of correlation spectroscopy, namely time-domain information, 2CG-FCS includes the direct determination of molecular concentration and brightness. It accounts for effects common to FRET measurements such as photobleaching, cross talk, and concentration variations. The molecule parameters of this assay are in principle unfavorable for FCS analysis, because the diffusion coefficients of the involved species are undistinguishable. The temporal decay information thus does not enter as an additional characteristic parameter for the molecular resolution, and the molecular analysis is solely based on fluorescence amplitude analysis. FCS methods are, however, based on time-dependent information and usually not well adapted to fluctuation amplitude analysis. As in this case, the amplitude is extracted by extrapolation to correlation time 0. FIDA-based methods directly perform statistics on fluctuating amplitudes and are thus better suited for such analysis (which becomes obvious by the better statistical accuracy of 2D-FIDA in this work). A combination of both temporal decay and fluctuation amplitude analysis would make up an even better analysis tool. Despite this fact, the global FCS analysis succeeded in revealing an excellent molecular resolution. 2CG-FCS remarkably improved accuracy of correlation analysis without gaining complexity in theory or loosing analysis speed. Thus, 2CG-FCS demonstrates a step toward the development of analysis tools with optimized molecular resolution accuracy. Biological assays involving molecular species, which are separable in diffusion time and fluorescence brightness, would even further highlight the capability of 2CG-FCS.

It is shown that 2CG-FCS can be applied to measurement times <2 s with a very high statistical accuracy. This opens up the door to industrial applications, in particular high-throughput drug discovery or molecular sorting. Especially the capability of molecular resolution enables one to filter out

background signal, e.g., autofluorescence, a problem common in drug discovery (10) or in in vivo studies (18). The use of beam scanning additionally increases statistical accuracy and motivates to further lower measurement times, even for correlation analysis methods.

The application of fluctuation analysis tools in confocal microscopy necessitates nanomolar concentrations of fluorescent molecules, which in this study was achieved by 1000-fold dilution of the labeled substrate. An online measurement of this enzymatic reaction would therefore be impossible. Potential developments of focal confinement such as microstructures or ultrahigh resolution microscopy (79–81) would enable one to use much higher concentrations and, consequently, to monitor enzymatic reactions online. This opens up further potentials for the presented method to be applicable to various kinds of assays. Accordingly, future progress will focus on broadening the range of applications, as well as to further enhance the accuracy by coming up with more globally operating analysis tools, as already presented by the recently developed methods, fluorescence intensity multiple distribution analysis (41), fluorescence intensity and lifetime distribution analysis (82), or photon arrival-time interval distribution analysis (43).

The authors gratefully acknowledge Sonja Dröge, Ole Kadasch, and Henrik Knorr for excellent assistance, and Jay Jethwa and Hans Blom for critically reading the manuscript.

REFERENCES

1. Lakowicz, J. R. 1999. Principles of Fluorescence Spectroscopy. Plenum Press, New York, NY.
2. Ambrose, W. P., P. M. Goodwin, J. H. Jett, A. van Orden, H. J. Werner, and R. A. Keller. 1999. Single molecule fluorescence spectroscopy at ambient temperature. *Chem. Rev.* 99:2929–2956.
3. Deniz, A. A., T. A. Laurence, M. Dahan, D. S. Chemla, P. G. Schultz, and S. Weiss. 2001. Ratiometric single-molecule studies of freely diffusing biomolecules. *Annu. Rev. Phys. Chem.* 52:233–253.
4. Kulzer, F., and M. Orrit. 2004. Single-molecule optics. *Annu. Rev. Phys. Chem.* 55:585–611.
5. Moerner, W. E., and D. P. Fromm. 2003. Methods of single-molecule fluorescence spectroscopy and microscopy. *Rev. Sci. Instrum.* 74: 3597–3619.
6. Xie, X. S., and J. K. Trautmann. 1998. Optical studies of single molecules at room temperature. *Annu. Rev. Phys. Chem.* 49:441–480.
7. Rigler, R., and E. L. Elson, editors. 2001. Fluorescence Correlation Spectroscopy: Theory and Applications. Springer, Berlin and Heidelberg, Germany.
8. Magde, D., E. L. Elson, and W. W. Webb. 1972. Thermodynamic fluctuations in a reacting system: measurements by fluorescence correlation spectroscopy. *Phys. Rev. Lett.* 29:705–708.
9. Meseth, U., T. Wohland, R. Rigler, and H. Vogel. 1999. Resolution of fluorescence correlation measurements. *Biophys. J.* 76:1619–1631.
10. Jäger, S., L. Brand, and C. Eggeling. 2003. New Fluorescence Techniques for High-Throughput Drug Discovery. *Curr. Pharm. Biotechnol.* 4:463–476.
11. Palmer, A. G., and N. L. Thompson. 1987. Molecular aggregation characterized by high order autocorrelation in fluorescence correlation spectroscopy. *Biophys. J.* 52:257–270.
12. Qian, H., and E. L. Elson. 1990. On the analysis of high order moments of fluorescence fluctuations. *Biophys. J.* 57:375–380.
13. Chen, Y., J. D. Müller, P. T. C. So, and E. Gratton. 1999. The photon counting histogram in fluorescence fluctuation spectroscopy. *Biophys. J.* 77:553–567.
14. Kask, P., K. Palo, D. Ullmann, and K. Gall. 1999. Fluorescence-intensity distribution analysis and its application in biomolecular detection technology. *Proc. Natl. Acad. Sci. USA.* 96:13756–13761.
15. Klumpp, M., A. Scheel, E. Lopez-Calle, M. Busch, K. J. Murray, and A. J. Pope. 2001. Ligand binding to transmembrane receptors on intact cells or membrane vesicles measured in a homogeneous 1-microliter assay format. *J. Biomol. Screen.* 6:159–170.
16. Van Rompaey, E., Y. Chen, J. D. Müller, E. Gratton, E. Van Craenenbroeck, Y. Engelborghs, S. De Smedt, and J. Demeester. 2001. Fluorescence fluctuation analysis for the study of interactions between oligonucleotides and polycationic polymers. *Biol. Chem.* 382:379–386.
17. Chirico, G., S. Bettati, A. Mozzarelli, Y. Chen, J. D. Müller, and E. Gratton. 2001. Molecular Heterogeneity of *O*-acetylserine sulfhydrylase by two-photon excited fluorescence fluctuation spectroscopy. *Biophys. J.* 80:1973–1985.
18. Chen, Y., J. D. Müller, Q. Ruan, and E. Gratton. 2002. Molecular brightness characterization of EGFP in vivo by fluorescence fluctuation spectroscopy. *Biophys. J.* 82:133–144.
19. Haupts, U., M. Rüdiger, S. Ashman, S. Turconi, R. Bingham, C. Wharton, P. J. Hutchinson, C. Carey, K. J. Moore, and A. Pope. 2003. Single molecule detection technologies in miniaturized high throughput screening: fluorescence intensity distribution analysis. *J. Biomol. Screen.* 8:19–33.
20. Gribbon, P., S. Schaertl, M. Wickenden, G. Williams, R. Grimley, F. Stühmeier, H. Preckel, C. Eggeling, J. Kraemer, J. Everett, W. W. Keighley, and A. Sewing. 2004. Experience in implementing uHTS: cutting edge technology meets the real world. *Curr. Drug Discovery Techn.* 1:27–35.
21. Fries, J. R., L. Brand, C. Eggeling, M. Köllner, and C. A. M. Seidel. 1998. Quantitative identification of different single-molecules by selective time-resolved confocal fluorescence spectroscopy. *J. Phys. Chem. A.* 102:6601–6613.
22. Ricka, J., and T. Binkert. 1989. Direct measurement of a distinct correlation function by fluorescence cross correlation. *Phys. Rev. A.* 39: 2646–2652.
23. Schwille, P., F. J. Meyer-Almes, and R. Rigler. 1997. Dual-color fluorescence cross-correlation spectroscopy for multicomponent diffusional analysis in solution. *Biophys. J.* 72:1878–1886.
24. Kask, P., K. Palo, N. Fay, L. Brand, Ü. Mets, D. Ullmann, J. Jungmann, J. Pschorr, and K. Gall. 2000. Two-dimensional fluorescence intensity distribution analysis: theory and applications. *Biophys. J.* 78:1703–1713.
25. Chen, Y., M. Tekmen, L. Hillesheim, J. Skinner, B. Wu, and J. D. Müller. 2005. Dual-color photon-counting histogram. *Biophys. J.* 88: 2177–2192.
26. Berland, K. M. 2004. Detection of specific DNA sequences using dual-color two-photon fluorescence correlation spectroscopy. *J. Biotechnol.* 108:127–136.
27. Heinze, K. G., A. Koltermann, and P. Schwille. 2000. Simultaneous two-photon excitation of distinct labels for dual-color fluorescence cross-correlation analysis. *Proc. Natl. Acad. Sci. USA.* 97:10377–10382.
28. Hwang, L. C., and T. Wohland. 2004. Dual-color fluorescence cross-correlation spectroscopy using single laser wavelength excitation. *Chem. Phys. Chem.* 5:549–551.
29. Kettling, U., A. Koltermann, P. Schwille, and M. Eigen. 1998. Real-time enzyme kinetics monitored by dual-color fluorescence cross-correlation spectroscopy. *Proc. Natl. Acad. Sci. USA.* 95:1416–1420.
30. Kim, H. D., G. U. Nienhaus, T. Ha, J. W. Orr, J. R. Williamson, and S. Chu. 2002. $Mg2^{+}$-dependent conformational change of RNA studied by fluorescence correlation and FRET on immobilized single molecules. *Proc. Natl. Acad. Sci. USA.* 99:4284–4289.

31. Merkle, D., S. P. Lees-Miller, and D. T. Cramb. 2004. Structure and dynamics of lipoplex formation examined using two-photon fluorescence cross-correlation spectroscopy. *Biochemistry*. 43:7263–7272.
32. Patel, R. C., U. Kumar, D. C. Lamb, J. S. Eid, M. Rocheville, M. Grant, A. Rani, T. Hazlett, S. C. Patel, E. Gratton, and Y. C. Patel. 2002. Ligand binding to somatostatin receptors induces receptor-specific oligomer formation in live cells. *Proc. Natl. Acad. Sci. USA*. 99:3294–3299.
33. Qian, H., and E. L. Elson. 2004. Fluorescence correlation spectroscopy with high-order and dual-color correlation to probe nonequilibrium steady states. *Proc. Natl. Acad. Sci. USA*. 101:2828–2833.
34. Rigler, R., Z. Földes-Papp, F. J. Meyer-Almes, C. Sammet, M. Völcker, and A. Schnetz. 1998. Fluorescence cross-correlation: a new concept for polymerase chain reaction. *J. Biotechnol*. 63:97–109.
35. Rippe, K. 2000. Simultaneous binding of two DNA duplexes to the NtrC-enhancer complex studied by two-color fluorescence cross-correlation. *Biochemistry*. 39:2131–2139.
36. Xia, K.-Q., Y.-B. Xin, and P. Tong. 1995. Dual-beam incoherent cross-correlation spectroscopy. *J. Opt. Soc. Am. A*. 12:1571–1578.
37. Bieschke, J., A. Giese, W. Schulz-Schaeffer, I. Zerr, S. Poser, M. Eigen, and H. Kretzschmar. 2000. Ultrasensitive detection of pathological prion protein aggregates by dual-color scanning for intensely fluorescent targets. *Proc. Natl. Acad. Sci. USA*. 97:5468–5473.
38. Eggeling, C., L. Brand, and S. Jäger. 2003. Highly sensitive fluorescence detection technology currently available for HTS. *Drug Discov. Today*. 8:632–641.
39. Twist, C. R., M. K. Winson, J. J. Rowland, and D. B. Kell. 2004. Single-nucleotide polymorphism detection using nanomolar nucleotides and single-molecule fluorescence. *Anal. Biochem.* 327:35–44.
40. Wright, P. A., H. F. Boyd, R. C. Bethell, M. Busch, P. Gribbon, J. Kraemer, E. Lopez-Calle, T. H. Mander, D. Winkler, and N. Benson. 2002. Development of a 1-μl scale assay for mitogen-activated kinase kinase 7 using 2-D fluorescence intensity distribution analysis anisotropy. *J. Biomol. Screen*. 7:419–428.
41. Palo, K., Ü. Mets, S. Jäger, P. Kask, and K. Gall. 2000. Fluorescence intensity multiple distribution analysis. Concurrent determination of diffusion times and molecular brightness. *Biophys. J*. 79:2858–2866.
42. Müller, J. D., Y. Chen, and E. Gratton. 2000. Resolving heterogeneity on the single molecule level with the photon-counting histogram. *Biophys. J*. 82:133–144.
43. Laurence, T. A., A. N. Kapanidis, X. Kong, D. S. Chemla, and S. Weiss. 2004. Photon arrival-time interval distribution (PAID): a novel tool for analyzing molecular interactions. *J. Phys. Chem. B*. 108:3051–3067.
44. Widengren, J., Ü. Mets, and R. Rigler. 1995. Fluorescence correlation spectroscopy of triplet states in solution: a theoretical and experimental study. *J. Phys. Chem*. 99:13368–13379.
45. Berland, K., P. T. C. So, Y. Chen, W. W. Mantulin, and E. Gratton. 1996. Scanning two-photon fluctuation correlation spectroscopy: particle counting measurements for detection of molecular aggregates. *Biophys. J*. 71:410–420.
46. Chen, Y., J. D. Müller, S. Y. Tetin, J. D. Tyner, and E. Gratton. 2000. Probing ligand protein binding equilibria with fluorescence fluctuation spectroscopy. *Biophys. J*. 79:1074–1084.
47. Förster, T. 1948. Zwischenmolekulare Energiewanderung und Fluoreszenz. *Ann. Phys*. 2:55–75. [in German].
48. Andrews, D. L., and A. A. Demidov. 1999. Resonance Energy Transfer. D. L. Andrews and A. A. Demidov, editors. John Wiley & Sons, Chicester, UK.
49. Clegg, R. M. 1992. Fluorescence resonance energy transfer and nucleic acids. *Methods Enzymol*. 211:353–388.
50. Ha, T. 2001. Single-molecule fluorescence resonance energy transfer. *Methods*. 25:78–86.
51. Jares-Erijman, E. A., and T. M. Jovin. 2003. FRET imaging. *Nat. Biotechnol*. 21:1387–1395.
52. Sekar, R. B., and A. Periasamy. 2003. Fluorescence resonance energy transfer (FRET) microscopy imaging of live cell protein localization. *J. Cell Biol*. 160:629–633.
53. Van Der Meer, B. W., G. I. Coker, and S. Y. S. Chen. 1994. Resonance Energy Transfer: Theory and Data. VCH Publishers, New York, NY.
54. Brasselet, S., E. J. G. Peterman, A. Miyawaki, and W. E. Moerner. 2000. Single-molecule fluorescence resonant energy transfer in calcium concentration dependent cameleon. *J. Phys. Chem. B*. 104:3676–3682.
55. Haas, E., and I. Z. Steinberg. 1984. Intramolecular dynamics of chain molecules monitored by fluctuations in efficiency of excitation energy transfer. *Biophys. J*. 46:429–437.
56. Horn, E. F. Y., and A. S. Verkman. 2002. Analysis of coupled bimolecular reaction kinetics and diffusion by two-color fluorescence correlation spectroscopy: enhanced resolution of kinetics by resonance energy transfer. *Biophys. J*. 83:533–546.
57. Kohl, T., K. G. Heinze, R. Kuhlemann, A. Koltermann, and P. Schwille. 2002. A protease assay for two-photon crosscorrelation and FRET analysis based solely on fluorescent proteins. *Proc. Natl. Acad. Sci. USA*. 99:12161–12166.
58. Widengren, J., E. Schweinberger, S. Berger, and C. A. M. Seidel. 2001. Two new concepts to measure fluorescence resonance energy transfer via fluorescence correlation spectroscopy: theory and experimental realizations. *J. Phys. Chem*. 105:6851–6866.
59. Margittai, M., J. Widengren, E. Schweinberger, G. F. Schröder, S. Felekyan, E. Haustein, M. König, D. Fasshauer, H. Grubmüller, R. Jahn, and C. A. M. Seidel. 2003. Single-molecule fluorescence resonance energy transfer reveals a dynamic equilibrium between closed and open conformations of syntaxin 1. *Proc. Natl. Acad. Sci. USA*. 100:15516–15521.
60. Hedstrom, L. 1996. Trypsin: a case study in the structural determinants of enzyme specificity. *Biol. Chem*. 377:465–470.
61. Perona, J. J., and C. S. Craik. 1995. Structural basis of substrate specificity in the serine proteases. *Protein Sci*. 4:337–360.
62. Grahn, S., D. Ullmann, and H.-D. Jakubke. 1998. Design and synthesis of fluorogenic trypsin peptide substrates based on resonance energy transfer. *Anal. Biochem*. 265:225–231.
63. Cornish-Bowden, A. 2004. Fundamentals of Enzyme Kinetics. Portland Press, London, UK.
64. Eggeling, C., S. Jäger, D. Winkler, and P. Kask. 2005. Comparison of different fluorescence fluctuation methods for their use in FRET assays. Monitoring a protease reaction. *Curr. Pharm. Biotechnol*. In press.
65. Heinze, K. G., M. Rarbach, M. Jahnz, and P. Schwille. 2002. Two-photon fluorescence coincidence analysis: rapid measurements of enzyme kinetics. *Biophys. J*. 83:1671–1681.
66. Magde, D., W. W. Webb, and E. L. Elson. 1978. Fluorescence correlation spectroscopy. III. Uniform translation and laminar flow. *Biopolymers*. 17:361–376.
67. Palmer, A. G., and N. L. Thompson. 1987. Theory of sample translation in fluorescence correlation spectroscopy. *Biophys. J*. 51:339–343.
68. Petersen, N. O. 1986. Scanning fluorescence correlation spectroscopy. I. Theory and simulation of aggregation measurements. *Biophys. J*. 49:809–815.
69. Ruan, Q., M. A. Cheng, M. Levi, E. Gratton, and W. W. Mantulin. 2004. Spatial-temporal studies of membrane dynamics: scanning fluorescence correlation spectroscopy (SFCS). *Biophys. J*. 87:1260–1267.
70. Winkler, T., U. Kettling, A. Koltermann, and M. Eigen. 1999. Confocal fluorescence coincidence analysis: an approach to ultra high throughput screening. *Proc. Natl. Acad. Sci. USA*. 96:1375–1378.
71. Kask, P., C. Eggeling, K. Palo, Ü. Mets, M. Cole, and K. Gall. 2002. Fluorescence intensity distribution analysis (FIDA) and related fluorescence fluctuation techniques: theory and practice. *In* Fluorescence Spectroscopy, Imaging and Probes: New Tools in Chemical, Physical and Life Sciences. R. Kraayenhof, A. J. W. G. Visser, and H. C. Gerritsen, editors. Springer, New York, NY. 153–181.
72. Kurth, T., S. Grahn, M. Thormann, D. Ullmann, H.-J. Hofmann, H.-D. Jakubke, and L. Hedstrom. 1998. Engineering the S1′ subsite of

trypsin: design of a protease which cleaves between dibasic residues. *Biochemistry*. 37:11434–11440.

73. Eggeling, C., J. Widengren, R. Rigler, and C. A. M. Seidel. 1999. Photostabilities of fluorescent dyes for single-molecule spectroscopy: mechanisms and experimental methods for estimating photobleaching in aqueous solution. *In* Applied Fluorescence in Chemistry, Biology and Medicine. W. Rettig, B. Strehmel, M. Schrader, and H. Seifert, editors. Springer, Berlin, Germany. 193–240.
74. Eggeling, C., J. Widengren, R. Rigler, and C. A. M. Seidel. 1998. Photobleaching of fluorescent dyes under conditions used for single-molecule-detection: evidence of two-step photolysis. *Anal. Chem*. 70:2651–2659.
75. Eggeling, C. 1999. Analyse von photochemischer Kinetik und Moleküldynamik durch mehrdimensionale Einzelmolekül-Fluoreszenzspektroskopie. PhD thesis. Georg-August-Universität Göttingen, Göttingen, Germany. [in German].
76. Zhang, J. H., T. D. Chung, and K. R. Oldenburg. 1999. A simple statistical parameter for use in evaluation and validation of high throughput screening assays. *J. Biomol. Screen*. 7:275–290.
77. Deniz, A. A., M. Dahan, J. R. Grunwell, T. Ha, A. E. Faulhaber, D. S. Chemla, S. Weiss, and P. G. Schultz. 1999. Single-pair fluorescence resonance energy transfer on freely diffusing molecules: observation of Förster distance dependence and subpopulations. *Proc. Natl. Acad. Sci. USA*. 96:3670–3675.
78. Schuler, B., E. A. Lipman, and W. A. Eaton. 2002. Probing the free energy surface for protein folding with single molecule fluorescence spectroscopy. *Nature*. 419:743–747.
79. Hell, S. W. 2003. Toward fluorescence nanoscopy. *Nat. Biotechnol.* 21:1347–1355.
80. Levene, M. J., J. Korlach, S. W. Turner, M. Foquet, H. G. Craighead, and W. W. Webb. 2003. Zero-mode waveguides for single-molecule analysis at high concentrations. *Science*. 299:682–686.
81. Laurence, T. A., and S. Weiss. 2003. How to detect weak pairs. *Science*. 299:667–668.
82. Palo, K., L. Brand, C. Eggeling, S. Jäger, P. Kask, and K. Gall. 2002. Fluorescence intensity and lifetime distribution analysis: toward higher accuracy in fluorescence fluctuation spectroscopy. *Biophys. J*. 83: 605–618.